Environ Earth Sci
DOI 10.1007/s12665-014-3374-7

ORIGINAL ARTICLE

Geospatial comparison of four models to predict soil erodibility in a semi-arid region of Central India

Partha Pratim Adhikary · S. P. Tiwari · Debashis Mandal · Brij Lal Lakaria · M. Madhu

Received: 29 October 2013 / Accepted: 21 May 2014

Abstract The soil erodibility factor of RUSLE is one of the important indicators of land degradation. It can be measured either directly under natural or simulated rainfall condition or indirectly estimated by empirical models. A geospatial variation of this factor is essential for prioritization of reclamation measures. However, geospatial upscaling of soil erodibility factor is very uncertain because of its dynamic nature and dependent on the parameters used in the model. This paper studies the geospatial comparison of the effectiveness of four different models to predict the soil erodibility factor by means of the independent role of each model parameter. 669 soil samples were collected from different land uses of Central India on grid basis and analyzed for physicochemical properties. The soil erodibility factor was estimated using four different models. Geostatistical analysis was performed on the point erodibility data of each model to obtain the spatial pattern. Analysis of variance showed that soil properties and erodibility factor varied significantly with various land uses. Croplands showed higher susceptibility to erosion than woodlands and grasslands. The erodibility equation that used particle size with soil organic matter showed better agreement with the variation of land use than the equation used only particle size. Therefore, the models that dynamically integrate soil intrinsic properties with land use can successfully be used for geospatial upscaling of soil erodibility factor.

Keywords Geospatial analysis · GIS · Land use · Soil erodibility factor

P. P. Adhikary (✉) · M. Madhu
Central Soil and Water Conservation Research and Training Institute, Research Centre, Sunabeda, Koraput 763 002, Odisha, India
e-mail: ppadhikary@gmail.com

S. P. Tiwari
Central Soil and Water Conservation Research and Training Institute, Research Centre, Gwalior Road, Datia 475 661, Madhya Pradesh, India

D. Mandal
Central Soil and Water Conservation Research and Training Institute, 218 Kaulagarh Road, Dehradun 248 195, Uttarakhand, India

B. L. Lakaria
Indian Institute of Soil Science, Nabibagh, Berasia Road, Bhopal, India

Introduction

Soil erosion is a natural process to maintain the balance between different ecosystem functionaries. However, accelerated-soil-erosion-led-land-degradation, due to non-environmental friendly anthropogenic activities, raises a major concern among the scientists and policy makers (Bathrellos et al. 2012, 2013; Klein et al. 2013; Youssef and Maerz 2013). Moreover, soils are often exposed to erosion due to faulty agricultural practices, deforestation, overgrazing, forest fires and urbanization (Terranova et al. 2009). In a semi-arid region, such as Bundelkhand in Central India, it is viewed as a serious problem, creating negative impact on agricultural production, infrastructure and water quality (Singh and Phadke 2006). Undoubtedly, soil erosion is the most extensive process of land degradation in arid and semi-arid regions of the world (Seager et al. 2007; Ravi et al. 2010).

Best management practices of land resources are essential to minimize the threat of soil erosion and to maintain the sustainability of the production. Quantitative

Published online: 06 June 2014

assessment of land degradation can be possible by various approaches using detailed and spatially distributed data. There are numerous mathematical and process based models to predict soil erosion (Smith et al. 1995; Botterweg et al. 1998; Sparovek et al. 2000), but the Revised Universal Soil Loss Equation (RUSLE) (Renard et al. 1997) is most widely used. It is simple, easy to use and successfully integrate the ecosystem parameters. In RUSLE, one of the important parameters is soil erodibility factor (K), which varies spatially under different land uses (Bayramin et al. 2008).

Many empirical models are there to determine the *K* factor of RUSLE based on geomorphological and soil physicochemical parameters, but the selection of a model for spatial simulation is very important. For a complex physical model, the data requirement would be too large. Moreover, if a complex model is applied with few data points, and a large part of the area is simulated with data assumed to be constant over a certain part of the area, the results may be very unreliable (Nearing 2005). Therefore, simple models are always better.

Torri et al. (1997) investigated the predictability of *K* factor from soil clay content, the Naperian logarithm of geometric mean particle diameter (Dg) and organic matter (OM). Romkens et al. (1986) used a function, based on particle size distribution (PSD) and four regression coefficients to calculate the *K* factor. Wischmeir and Smith (1978) used soil texture, structure, organic matter and soil profile permeability to predict *K* factor. Mulengera and Payton (1999) developed an equation to predict *K* factor for the soils of tropical condition using soil texture, OM and soil permeability data. All the models determine the *K* factor with varying degree of perfection. However, they cannot provide spatial distribution of soil erosion due to the constraint of limited samples in complex environments. Therefore, model selection to map soil erosion over large areas is often very difficult (Lu et al. 2004).

Recently, Geographic Information System (GIS) and geostatistics have widely been used in soil science to predict soil salinity (Douaik et al. 2005), soil hydraulic properties (Herbst et al. 2006), soil organic matter (Chai et al. 2008) and soil erosion (Saygm et al. 2014). To predict soil erosion, combined use of USLE/RUSLE and GIS is common (Lee 2004; Prasannakumar et al. 2011; Rozos et al. 2013; Perovic et al. 2013). However, the spatial prediction of *K* factor is very uncertain.

To overcome the uncertainty to predict *K* factor over space, sequential Gaussian simulation (Baskan et al. 2010), joint sequential simulation (Parysow et al. 2003) and geostatistical simulation (Castrignano et al. 2008) may be the options. Geostatistical simulation, as compared to an optimal procedure of estimation, provides a more realistic means of evaluating spatial variability of a variable (Castrignano et al. 2008). This results in a large number of equiprobable images (also called realizations) that honour the sample data and reproduce statistical characteristics and spatial features. Buttafuoco et al. (2012) quantified the output error of a soil erodibility model, resulting from uncertainties in the model inputs, to contribute towards an overall uncertainty analysis of soil loss prediction.

K factor is not static, but highly dynamic. It accounts for the effect of different intrinsic soil properties on erosion (Wang et al. 2001), thereby dynamically linked with climate, topography, vegetation, relief and time. Therefore, prediction of the spatial distribution of *K* factor is very uncertain and its geospatial upscaling is very sensitive. Hence, the consistency of any model to predict *K* factor, and its upscaling by geospatial analysis relies mainly on its performance to represent characteristic exchanges of the mineralogical, physical, chemical, and biological soil processes within an ecosystem (Saygm et al. 2011).

The quantification of spatial variation of soil erodibility factor depends not only on external factors like land use/cover, climate, topography, but also on the intrinsic properties of soils that promote their resistance to erosion (Singh and Khera 2009). The main soil properties that control this factor include particle size distribution, shape, size and stability of aggregates, shear strength, bulk density, porosity and permeability, organic matter and clay content, and chemical composition (Morgan 1995; Chen and Zhou 2013). These properties vary with space and time. Therefore, the models which include these properties to calculate *K* factor are prone to severe limitations during geospatial prediction of *K* factor.

The geospatial prediction of the *K* factor should vary depending on the differences in ecosystem functions over a research area, and therefore, any equation for estimating it should have dynamic and interactive variables to account for changing land properties (Saygm et al. 2011). There are number of studies available to predict geospatial variation of *K* factor using GIS. However, the spatial comparison of predicting models over a large area is very rare. The objective of the study is to geospatial comparison of the effectiveness of four different models to predict the *K* factor by means of the independent role of each model parameter.

Materials and methods

Study area

The study area, Bundelkhand region, straddling over 7.07 M ha in Central India, lies between 23°10′ and 26°30′ north latitude and 78°20′ and 81°40′ east longitude,

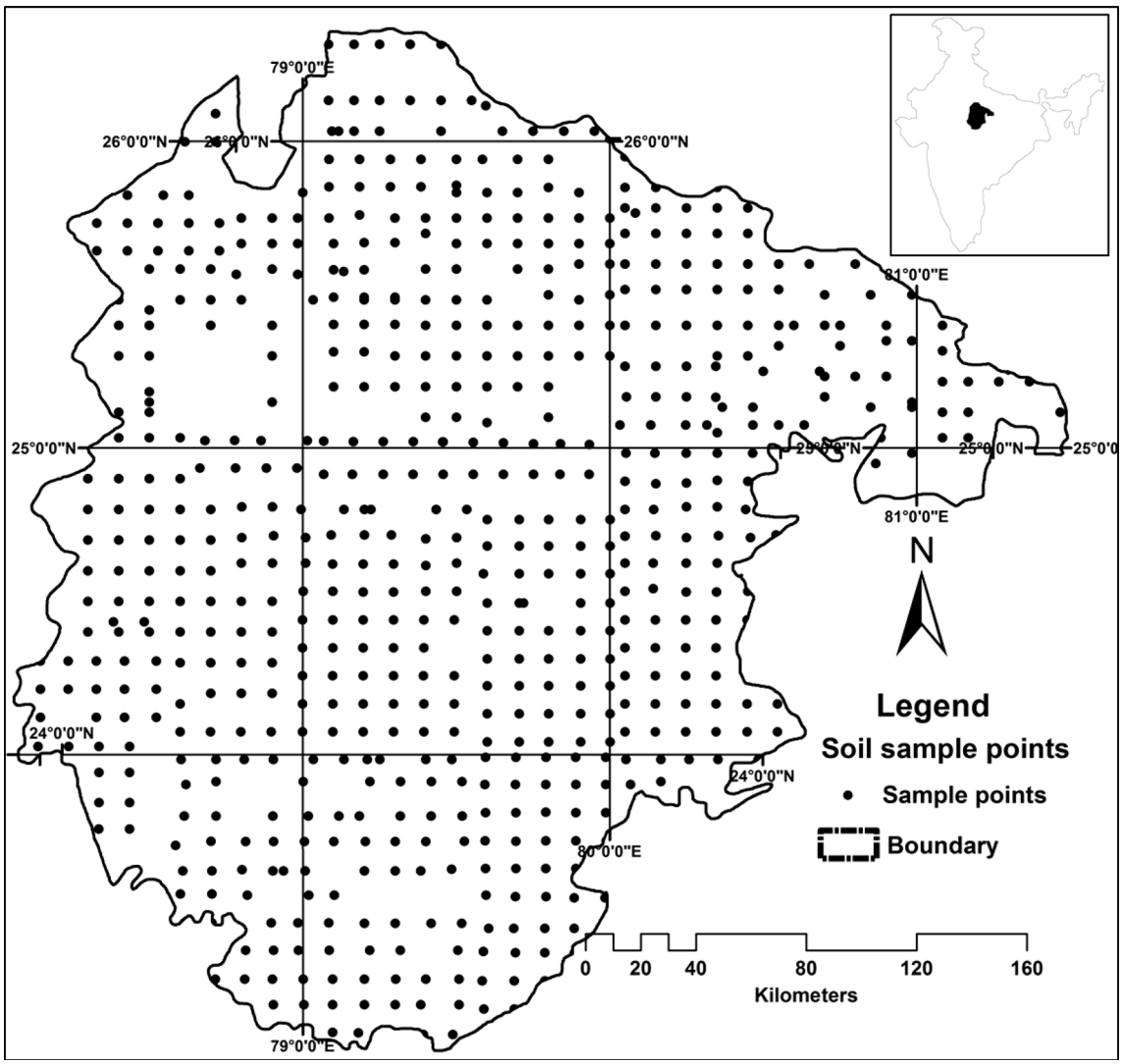

Fig. 1 Map of the study area showing the location of soil sampling points

comprises seven districts of Uttar Pradesh and six districts of Madhya Pradesh (Fig. 1). It has been recognized as one of the most degraded and threatened eco-systems of the country (Ratha Krishnan 2008). The climate is tropical and semi-arid with average annual rainfall ranges from 750 mm in the north-west to 1,250 mm in the south-east. More than 94 % of the rainfall occurs between June and September, with maximum during July–August. Rainfall intensity often goes up to 30–50 mm per hour. Thus rain water has little time to infiltrate, and aggravates the problem of soil erosion and poor groundwater recharge. The temperature varies from −1.5 to 49 °C with hottest days are in May and coldest days in December or January. The land use of Bundelkhand is mainly classified as croplands, fallowlands, woodlands and grasslands with few subclasses. In north Bundelkhand, the area under croplands is significantly higher than the south, whereas the south Bundelkhand comprises significant amount of woodlands.

Geology and topography

Granites of varying types from the lower Pre-Cambrian/Archaen period are the predominant geological materials found across the region. These are followed by gneisses and sedimentary strata, such as sandstone and limestone. Alluvial deposits of clay, silt and sand of sub-aerial and fluviatile origin are the most recent geological deposits in Bundelkhand, and are more predominant near the *Yamuna* river and its tributaries. The topography is generally undulating with rocky outcrops and boulder-strewn plains that give the landscape a rugged look. Spectacular ravines in the north and deep gorges in the south are the result of the active erosion of the unconsolidated alluvial material deposited by the major streams in the region; namely the *Betwa*, *Dhasan* and the *Ken*. These ravines and gorges are uncultivable and pose an increasing threat to nearby farmland as they continue to expand.

Soils

The soils have been developed from Vindhyan rocks abounding in gneiss and granites of the Deccan trap with highly ferruginous beds and often limestones. The soils are broadly divided into two main groups, red and black, further subdivided as *Rakar*, *Parua*, *Kabar* and *Mar* (Tiwari and Narayan 2010). Red soils have developed over granite and gneiss parent material and they exist mostly on uplands. Taxonomically, the soils are covered under the order Alfisol and Entisol. The *Rakar* soils are residual, slightly acidic, gravelly, shallow and excessively permeable with low water holding capacity. The *Parua* soils are alluvial and mildly alkaline with moderate water holding capacity and fertility status. The black soils *Mar* and *Kabar* are very deep and confined to low lying landscape, possess fine texture and exhibit swell–shrink property. The *Mar* soils pose drainage and workability problems. These soils belong to the orders Inceptisol and Vertisol.

Soil sampling and physicochemical analysis

669 surface (0–15 cm depth) soil samples (Fig. 1) were used for this study. Geographical coordinates and elevation of each sampling location was recorded using a handheld global positioning system (GPS). A few locations were also cross-checked with a differential GPS. Soil samples were analyzed for sand (S), silt (Si) and clay (C) content by international pipette method (Piper 1966). Coarse and fine sand content was estimated by wet sieving through 0.1 mm screen openings (Soil Survey Staff 1996). The method of Walkley and Black (1934) was used to determine soil organic carbon (SOC). Hydraulic conductivity was calculated from the values recorded under saturated conditions with a constant head permeameter (Klute and Dirksen 1986). Soil structure was determined by a field method (Soil Survey Staff 1996).

Soil erodibility models

Soil erodibility depends on the intrinsic properties of the soils. Many empirical models were developed to determine the *K* factor of RUSLE based on the geomorphological and soil physicochemical parameters. However, for this study, four equations by Romkens et al. (1986), Mulengera and Payton (1999), Wischmeir and Smith (1978) and Torri et al. (1997) were evaluated.

Romkens et al. (1986) used the published global data on particle size distribution to calculate the *K* factor in the form of the following equation ($R^2 = 0.983$).

$$K_1 = \propto + \beta \exp\left\{-\frac{1}{2}\left(\frac{\log D_g + \chi}{\gamma}\right)^2\right\} \quad (1)$$

where K_1 is the soil erodibility factor (t ha h ha^{-1} MJ^{-1} mm^{-1}), α, β, χ, and γ are the coefficient parameters. Romkens et al. (1986) used the parameter values of 0.0034, 0.0405, 1.659, and 0.7101 for α, β, χ, and γ, respectively. D_g is the geometric mean weight diameter of the primary soil particles (mm), which is calculated by the following equation:

$$D_g = 0.01 * \left\{\sum_{n=1}^{n}(f_i \ln m_i)\right\} \quad (2)$$

where f_i is the primary particle size fraction in percent (percent sand (S), silt (Si), and clay (C) with $i = 1$, 2 and 3, respectively) and m_i is the arithmetic mean of the particle size limits of the corresponding size (Shirazi and Boersma 1984).

The second model we used is the equation developed in the framework of a research program initiated to identify a suitable soil loss equation for use under tropical conditions (Mulengera and Payton 1999). This equation is based on the texture-derived parameters and soil permeability that were found to be quite adequate for estimating the soil erodibility factor in the tropics. The following equation developed by these authors obtained the best correlation coefficient ($r = 0.911$) between calculated and measured values in Tanzania.

$$K_2 = 1.82247 * 10^{-5} M + 0.0045 * P - 0.0097 \quad (3)$$

where K_2 is the soil erodibility factor (t ha h ha^{-1} MJ^{-1} mm^{-1}), M is the product of the primary particle size fractions [$M = (\text{si} + \text{vfs})\ (\text{si} + \text{vfs} + \text{s})$; si: percent silt (0.05–0.002 mm), s: percent sand (0.2–0.10 mm), vfs: percent very fine sand (0.10–0.05 mm)], P is the class of soil profile permeability.

The third equation we used in our study is the most famous and frequently used soil erodibility nomograph (Wischmeir and Smith 1978) stated as below:

$$K_3 = \frac{1}{759}\{2.1 * 10^{-4}(12 - SOM) * M^{1.14} + 3.25(S - 2) + 2.5(P - 3)\} \quad (4)$$

where K_3 is the soil erodibility factor (t ha h ha^{-1} MJ^{-1} mm^{-1}), *SOM* is percent soil organic matter content, M is the product of the primary particle size fractions [$M = (\text{si} + \text{vfs})\ (\text{si} + \text{vfs} + \text{s})$; si: percent silt (0.05–0.002 mm), s: percent sand (0.2–0.10 mm), vfs: percent very fine sand (0.10–0.05 mm)], S is soil structure code and P is permeability class (Renard et al. 1997).

The last equation used to determine K factor for our study is the equation of Torri et al. (1997):

$$K_4 = 0.0293 * \left(0.65 - D_g + 0.24D_g^2\right) * \exp\left\{-0.0021\left(\frac{SOM}{C}\right) - 0.00037\left(\frac{SOM}{C}\right)^2 - 4.02C + 1.72C^2\right\} \quad (5)$$

where K_4 is the soil erodibility factor (t ha h ha^{-1} MJ^{-1} mm^{-1}), SOM is the percent soil organic matter, C is the percent clay content and D_g is the decimal logarithm of the geometric mean of PSD, which is calculated using the following equation:

$$D_g = \sum_{i=1}^{n} f_i \times \log_{10}\left(\sqrt{d_i d_{i-1}}\right) \quad (6)$$

where f_i is the fraction of primary particles with sizes within d_i and d_{i-1} as defined by Shirazi et al. (1988).

The differences between Eqs. 1, 3, 4 and 5 are that, Eq. 1 used only particle size distribution (PSD) data to determine K factor, whereas Eq. 3 used soil profile permeability data besides PSD. The Eq. 4 used PSD, soil profile permeability and soil organic matter data to determine K factor, whereas Eq. 5 used PSD and SOM data, but not soil profile permeability. One of the disadvantages of the Eq. 4 is that the results could be unreliable when applied to soils with textural extremes as well as well aggregated or no erodible soils (Romkens et al. 1986). As, all the equations are dissimilar, their output values will be diverse for the same sampling point with their empirical lower and upper bounds obtained with different data sets. A basic understanding of how physical parameters used in these equations influence spatial patterns would ease the interpretation of the K factor of the study area (Saygm et al. 2011).

Geostatistical analysis

Kriging is the optimal approach for spatial interpolation at unsampled locations. It is flexible and permits the investigation of spatial autocorrelation of the variables. It presents the possibility of estimation of the interpolation error of the values of the regionalized variable, where there are no initial measurements. This feature offers a measure of the estimation accuracy and reliability of the spatial distribution of the variable. The spatial dependence is quantified using semivariogram (Burgess and Webster 1980). The semivariogram is mathematically described by the following equation (Journel and Huijbregts 1978):

$$\gamma(h) = \frac{1}{2N(h)} \sum_{i=1}^{N(h)} [z(x_i + h) - z(x_i)]^2 \quad (7)$$

where $\gamma(h)$ is the semivariogram expressed as a function of the magnitude of the lag distance or separation vector h between two points, $N(h)$ is the number of observation pairs separated by distance h and $z(x_i)$ is the random variable at location x_i. The experimental semivariogram $\gamma(h)$ is fitted with a theoretical model, such as spherical, exponential, linear, or Gaussian to determine three parameters, such as the nugget (C_0), the sill (C), and the range (A_0).

During calculation of experimental semivariogram values, maximum separation distance was fixed as half of the extent of the sampling area. The calculated experimental semivariogram values were then fitted in the spherical semivariogram model, which was found best during weighted least square fitting and described below:

$$\gamma(h) = c_0 + \left[1.5\left(\frac{h}{A_0}\right) - 0.5\left(\frac{h}{A_0}\right)^3\right] \quad h \le A_0$$
$$\gamma(h) = c_0 + c, \quad h > A_0 \quad (8)$$

where C_0 is the nugget variance, C is the sill variance, and A_0 is the range of distance parameter. Using this interpolation technique, spatial variation maps of the soil erodibility factor were prepared.

Spatial autocorrelation of soil erodibility factor

Variable, such as soil erodibility factor has discrete values measured at several locations can be considered as random. However, they show a certain degree of spatial correlation with themselves. Therefore, to know the randomness of the sample points, the arrangement pattern of the sampling points was analysed. Moreover, the spatial autocorrelation analysis was carried out using GS+ software to understand the correlation between the points for different shifts in space and to visualize the spatial variability of the K factor.

Development of semivariogram model and cross validation

The normality of each data-set was checked by Kolmogorov–Smirnov test and different transformations, such as log normal, square root were carried out to ensure normal distribution. Geostatistical software GS+ was used to generate the semivariogram parameters for each theoretical model. The best-fitted theoretical model was selected based on the highest R^2 and lowest RSS. The corresponding sill, nugget, and range values of the best-fitted theoretical models were observed (Fig. 2). Subsequently, thematic maps for K factor were generated using ordinary kriging.

The predictive performance of the fitted models was checked by cross-validation tests. The values of coefficient of determination R^2, mean absolute error (MAE), mean square error (MSE), kriged reduced mean error (KRME),

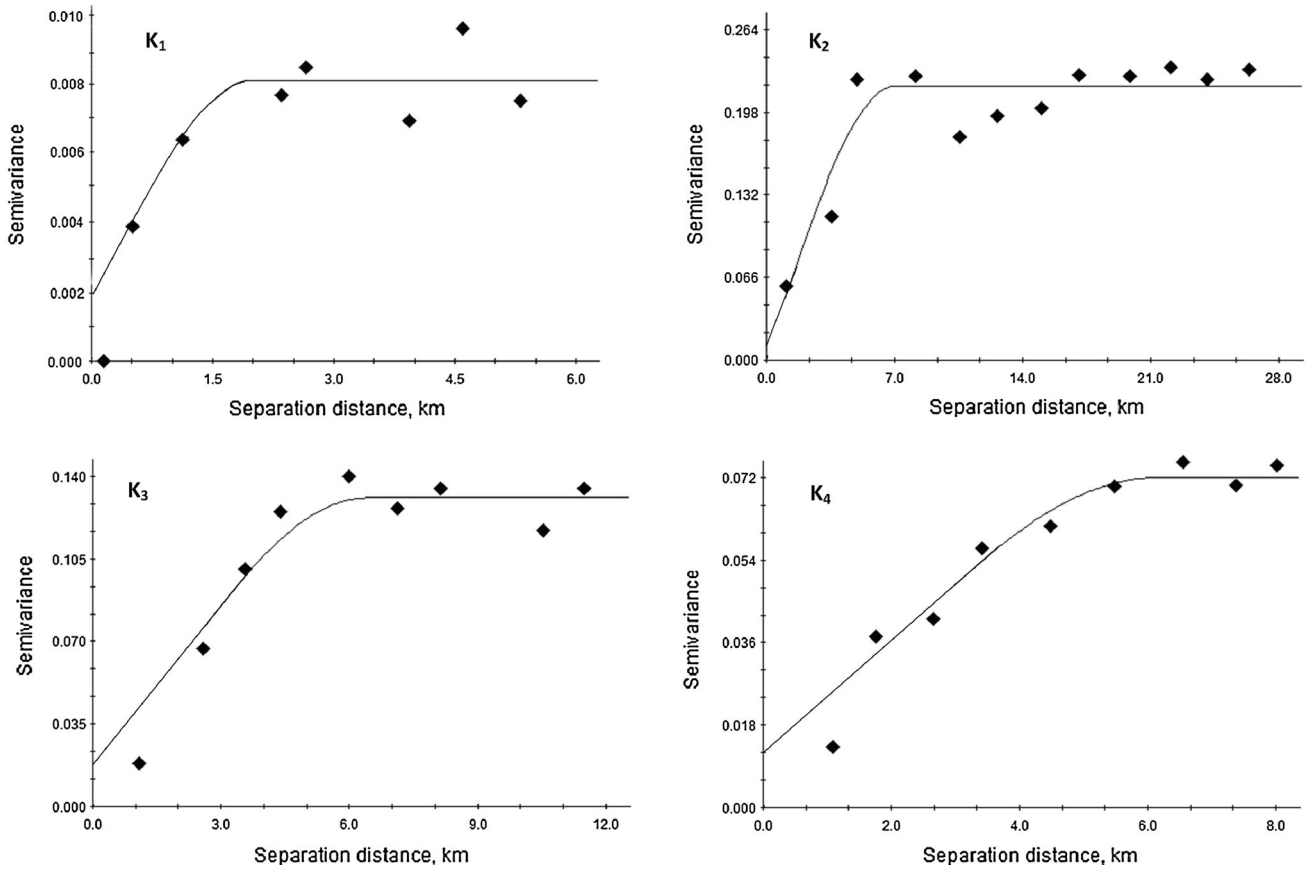

Fig. 2 Semivariograms of soil erodibility factor in the Bundelkhand region obtained using four different models

and kriged reduced mean square error (KRMSE) were estimated to ascertain the performance of the developed theoretical models (Sarangi et al. 2005). The predictive behaviors of the models were ascertained from the estimated values approaching 0 or 1, as indicated below:

$$R^2 = 1 - \frac{SS_{\mathrm{E}}}{SS_{\mathrm{T}}} \cong 1 \tag{9}$$

$$MAE = \frac{1}{N}\sum_{i=1}^{N}\left(Z_{o,i} - Z_{p,i}\right) \cong 0 \tag{10}$$

$$MSE = \frac{1}{N}\sum_{i=1}^{N}\left(Z_{\mathrm{o},i} - Z_{\mathrm{p},i}\right)^2 \cong \text{Minimum} \tag{11}$$

$$KRME = \frac{1}{N}\sum_{i=1}^{N}\frac{\left(Z_{\mathrm{o},i} - Z_{\mathrm{p},i}\right)}{S} \cong 0 \tag{12}$$

$$KRMSE = \frac{1}{N}\sum_{i=1}^{N}\frac{\left(Z_{o,i} - Z_{p,i}\right)^2}{S^2} \cong 1 \tag{13}$$

where $Z_{\mathrm{o},i}$ is the observed value at location i, $Z_{\mathrm{p},i}$ is the predicted value at location i, S^2 is the estimated variance and N is the number of pairs of observed and predicted values. *SSE* and *SST* are the error sum of square and total sum of square respectively. The ME and KRME values near to zero is an indicator of better model prediction.

Results and discussions

Descriptive statistics of different soil parameters and erodibility

Descriptive statistics of K factor calculated by different models along with their input parameters is presented in Table 1. The range, mean and standard deviation values showed considerable heterogeneity within the input parameters. Skewness and kurtosis, which measure the distribution symmetry and distribution flatness/steepness relative to a normal distribution, were checked to ascertain the normality of the data-set (Cerri et al. 2004). Coefficients of skewness and kurtosis for soil profile permeability (SPP) showed positively skewed and leptokurtic distribution. Kolmogorov and Smirnov test also indicated that all the data except SPP, to compute erodibility factor, were normally distributed at $p < 0.05$. The log transformation has transformed this distribution normal. CV is the first approximation of not only sampling site heterogeneity for

Table 1 Descriptive statistics of the soil erodibility factors (K_1, K_2, K_3 and K_4) and their input parameters

Parameter	Minimum	Maximum	Mean	SD	Skewness	Kurtosis	CV
Sand (%)	4.0	92.0	40.4	20.6	0.4	−0.7	51.0
Silt (%)	4.0	76.0	26.0	12.9	0.7	0.7	49.7
Clay (%)	2.0	73.0	33.6	15.3	−0.1	−1.1	45.6
SOM (%)	0.2	4.9	1.3	0.8	1.0	0.8	60.3
SPP (cm h^{-1})	1.2	79.9	6.3	9.4	6.6	48.8	147.8
K_1	0.0079	0.0439	0.0349	0.0095	−1.1	−0.1	27.4
K_2	0.0051	0.1229	0.0372	0.0201	1.3	2.5	54.1
K_3	0.0095	0.0932	0.0317	0.0137	1.4	3.2	43.2
K_4	0.0204	0.0642	0.0322	0.0073	1.5	2.7	22.6

SD standard deviation, *CV* coefficient of variation, *SOM* soil organic matter, *SPP* soil profile permeability

input parameters, but also the relative spatial distribution of the equations in the area. Permeability values of soil samples showed the highest CV (147.8 %). Relatively lower CV values were obtained for S, Si, C and SOM contents of the soil samples (51, 49.7, 45.6, and 60.3 %, respectively). Higher variation of permeability was mainly due to variation of land uses and management practices (Saygm et al. 2011), since significant decrease in permeability and SOM was observed in woodlands after their conversion to croplands. For the *K* factor calculating equations, relatively higher CVs were observed for K_2 (54.1 %) and K_3 (43.2 %) and lower for K_1 (27.4 %) and K_4 (22.6 %). The higher CV of K_2 and K_3 could be linked to the spatial variations of the input parameters of Eqs. 3 and 4. In both the equations, permeability was one of the input parameters. A noticeably higher variation in the permeability values of the soil samples interacted with those of other input parameters and resulted higher CV values of K_2 and K_3.

Variation of soil properties and erodibility among different land uses

Land use and soil texture

Table 2 shows the analysis of variance to compare the effect of different land uses on sand, silt, clay, SOM, SPP and RUSLE *K* factor. The result indicated that land use has profound influence on the variation of soil texture (Bayramin et al. 2008). Highest (54.6 %) and lowest (28.6 %) sand content was observed in grassland and fallowland, respectively; whereas cropland and woodland showed nearly a similar level of sand content. On the other hand, clay content variation showed the opposite trend that of sand. Highest (45.8 %) and lowest (29.3 %) clay content was observed in fallowland and grassland, respectively. The variation of clay content between cropland and woodland was statistically non-significant. The grasslands were under high pressure from growing cattle population and overgrazed, which induced accelerated soil erosion and subsequent washing out of clay and silt, leaving the sand particles in their original place (Tiwari and Narayan 2010). Thus, the grasslands showed highest sand and lowest clay content. With regards to the variation of silt content under different land uses, grassland showed the lowest (16.1 %) and fallowland, highest silt content (25.7 %). This can be explained by the fact that silt is the most susceptible soil particle size fraction for water erosion and the amount vary under various erosion circumstances. The fallowlands and croplands, because of their inherent higher silt content, were more sensitive to water erosion than woodland and grassland (Bayramin et al. 2008). On the other hand, due to overgrazing and high biotic pressure on grassland, the silt has already been eroded and hence showed its depletion in grassland. Under cropland, fallowland and woodland, the variation of silt content was statistically significant, but numerically very close (between 21.4 and 25.7 %) to each other. Thus, one can assume that an equilibrium condition has been attained among land uses from the viewpoint of erosion processes. Therefore, in terms of silt, the effect of textural composition on the sensitivity of soils to water erosion was similar in the ecosystem of the Bundelkhand region of Central India. In fact, the parent material and topography as soil-forming factors together with biotically influenced detachment, transport, and depositional processes could be considered as factors characterizing the textural composition of soils in the study area.

Land use and soil organic matter

Conversion of the woodland and fallowland to the cropland had a significant effect on the SOM in the study area. The SOM of cropland has been depleted by 17.3 and 6.5 % as compared to the woodland and fallowland, respectively. The cultivation detached soil aggregates and exposed previously inaccessible organic matter to microbial attack and accelerated the decomposition and mineralization of SOC (Shepherd et al. 2001). Incorporation of lesser amount of plant residues after harvest, continuous cropping and

Table 2 Analysis of variance (Mean ±SD) for soil properties and soil erodibility factors (K_1, K_2, K_3 and K_4) as affected by the different land uses ($p < 0.05$)

Parameter	Cropland	Fallow land	Woodland	Grassland
Sand (%)	$37.57^{C} \pm 1.07$	$28.56^{D} \pm 3.19$	$42.93^{B} \pm 1.68$	$54.61^{A} \pm 3.42$
Silt (%)	$23.64^{AB} \pm 0.44$	$25.67^{A} \pm 1.62$	$21.40^{BC} \pm 0.71$	$16.11^{D} \pm 1.42$
Clay (%)	$38.78^{BC} \pm 0.75$	$45.78^{A} \pm 3.11$	$35.67^{BC} \pm 1.13$	$29.29^{D} \pm 2.11$
SOM (%)	$1.58^{B} \pm 0.02$	$1.68^{B} \pm 0.04$	$1.91^{A} \pm 0.17$	$1.27^{C} \pm 0.07$
SPP (cm h^{-1})	$4.54^{C} \pm 0.19$	$3.24^{D} \pm 0.26$	$6.10^{B} \pm 0.34$	$8.07^{A} \pm 0.83$
K_1	$0.038^{B} \pm 0.001$	$0.041^{A} \pm 0.001$	$0.034^{C} \pm 0.001$	$0.031^{D} \pm 0.002$
K_2	$0.035^{A} \pm 0.001$	$0.034^{A} \pm 0.002$	$0.026^{B} \pm 0.001$	$0.022^{C} \pm 0.002$
K_3	$0.030^{A} \pm 0.001$	$0.029^{A} \pm 0.002$	$0.024^{B} \pm 0.001$	$0.023^{B} \pm 0.001$
K_4	$0.029^{A} \pm 0.001$	$0.028^{A} \pm 0.001$	$0.030^{A} \pm 0.001$	$0.030^{A} \pm 0.001$

Uppercase letters indicate statistically significant differences among soil properties affected by the different land uses

SD standard deviation, *SOM* soil organic matter, *SPP* soil profile permeability

Table 3 Pearson's correlation coefficients among sand, silt, clay, SOM and SPP for each land use type

	Sand	Silt	Clay	SOM	SPP
Woodland					
Sand	1				
Silt	−0.85*	1			
Clay	−0.94*	0.63*	1		
SOM	−0.10	0.14	0.06	1	
SPP	0.96*	−0.89*	−0.86*	−0.16	1
Cropland					
Sand	1				
Silt	−0.827*	1			
Clay	−0.943*	0.592*	1		
SOM	0.005	−0.039	0.016	1	
SPP	0.894*	−0.822*	−0.794*	−0.048	1
Fallowland					
Sand	1				
Silt	−0.306	1			
Clay	−0.868*	−0.208	1		
SOM	−0.348	−0.231	0.478	1	
SPP	0.997*	−0.321	−0.857*	−0.373	1
Grassland					
Sand	1				
Silt	−0.952*	1			
Clay	−0.979*	0.869*	1		
SOM	0.274	−0.319	−0.229	1	
SPP	0.944*	−0.912*	−0.914*	0.257	1

SOM soil organic matter, *SPP* soil profile permeability

* $p < 0.05$

frequent burning, faster decomposition rates of organic matter, and greater erosion were the few reasons for declining nature of SOC in the croplands (Rezapour 2014). Furthermore, as a matter of fact, a variation of the SOC content could be affected with soil detachment, transport, and depositional processes, which could significantly result from the land use changes (Basaran et al. 2008). The analysis of Pearson's correlation indicated that there was a strong positive correlation between SOM and clay and negative correlation between SOM and sand in fallowland. Except these, SOM did not correlate with any other soil parameters (Table 3). Clay is an important soil parameter required for the accumulation and protection of SOM. However, except fallowland, there was no significant correlation between clay and SOM for other land use types. This indicated the fragile nature of the ecosystem of Bundelkhand region in terms of SOC.

Land use and soil permeability

The variation of SPP under different land uses followed the same trend as that of sand content. The grassland showed the highest (8.1 cm h^{-1}) and fallowland, lowest (3.2 cm h^{-1}) SPP; whereas, the SPP of cropland and woodland were 4.5 and 6.1 cm h^{-1}, respectively (Table 2). The high SPP of grassland may be attributed to the high sand content and loosening of surface soil by trampling of cattle, goat and sheep. Side by side, the fibrous root system of grass had made the system conducive for high permeability (Chen et al. 2009). The low SPP of fallowland may due to high clay content of the surface soil layer. Good correlations existed between SPP and sand, silt and clay for all the land uses. As usual, the SPP was positively correlated with sand content and negatively with clay and silt content (Table 3). This confirmed the fact that, in the study area, irrespective of the land use, sand was the governing factor to determine SPP. Interestingly, SOM, one of the important soil parameters governing the water movement within the soil, showed no significant correlation with SPP. This may be due to the presence of low amount of SOM in

the soils of the study area which practically lagged far behind the textural effect to control and make any significant impact on the SPP.

Land use and soil erodibility factor

Table 2 indicated that the soil erodibility factor (K) differed significantly among land uses ($p < 0.01$), but the degree of difference varied for different models used to determine the K factor. K_1, which depended on only PSD, varied significantly among all the land uses. The trend of variation of K_1 under different land uses exactly followed the same trend that of PSD. K_1 was directly proportional to the silt and clay content and inversely proportional to the sand content. In fallowland, the presence of highest silt and clay, and lowest sand content triggered the K_1 value to be highest and the inverse has been observed for grassland. The K_2, dependent on PSD and SPP, showed nearly the same trend as that of the K_1. The SPP was strongly correlated with PSD for all the land uses, therefore, the combine effect of PSD and SPP, as effervesced in K_2 followed a similar pattern as that of the K_1. For K_3, which was derived from PSD, SPP and SOM, grassland and woodland behaved similarly and cropland and fallowland behaved similarly. K_3 differed from K_2 only because it included SOM as one of the input parameters. Therefore, the importance of SOM to control the behavior of K factor was significant when we compared cropland with woodland. However, this importance has lost its significance when we compared woodland with grassland. In grassland, besides SOM, other factors like PSD, biogenic macropores and fibrous root systems of grasses played a significant role in determining the erosion potentiality of its soils (Basaran et al. 2008). On the other hand, K_4, which was derived from PSD and SOM showed statistically insignificant difference between different land uses. Overall, the K factors of croplands and fallowlands were higher than woodlands and grasslands. Continuous cultivation in croplands has made the land surfaces more vulnerable to water erosion. In contrast, fibrous root systems coupled with high coarser soil particles in the grasslands and higher sand and SOM content in the woodlands protect their soils from erosion (Bayramin et al. 2008). Therefore, it can be incurred that, input parameters of different soil erodibility models are dynamically related to each other, which vary spatially and temporally and influenced soil erodibility single and/or combined.

Table 4 Statistical summary of the Moran's I, the measure of spatial autocorrelation

Moran's I			
Parameter	Minimum	Maximum	Mean
Sand	−0.011	0.274	0.119
Silt	0.233	0.409	0.302
Clay	−0.098	0.216	0.026
SOM	0.127	0.418	0.195
SPP	−0.128	0.272	0.138
K_1	0.067	0.401	0.168
K_2	0.104	0.423	0.211
K_3	0.258	0.467	0.316
K_4	0.204	0.403	0.246

SOM soil organic matter, *SPP* soil profile permeability

Geospatial analysis

Spatial interdependence of different erodibility equations

Spatial autocorrelation measures the level of interdependence between different variables and the nature and strength of that interdependence. The probability of finding three, five, seven and nine other points within a specified distance of any point showed a linear growth with distance. The spatial autocorrelation coefficients or the Moran's I values for the four soil erodibility factors derived from four different models along with their input parameters are summarized in Table 4. The result indicated that sand, clay, SOM and SPP showed very week positive autocorrelation (average Moran's $I > 0$ but very close to zero), while silt showed weak to moderate positive autocorrelation. All the soil erodibility factors showed weak positive autocorrelation (average Moran's $I > 0$ but close to zero). Therefore, all the erodibility factors are independent of each other and near randomly distributed within the study area.

Spatial structure of soil erodibility factors

To ascertain normality of the data distribution, except for K_1, all other erodibility equations were transformed to square root distribution. The directional anisotropy of the semivariograms was checked and found that there was no severe directional anisotropy. Therefore, omni-directional semivariograms were obtained based on least square technique. The theoretical semivariogram models were examined and spherical model was considered as best-fit, because of highest R^2 value. The parameters of the best-fit spherical model for the K factors are given in Table 5. Nugget and sill were very low and varied from 0.002 to 0.018 and 0.008 to 0.219, respectively, for all the K factors. Nugget effect and nugget-to-sill ratio was also used to classify the spatial dependence (Cambardella et al. 1994) of the variable. The nugget-to-sill ratio indicated that all the soil erodibility equations were weakly spatially correlated. The range was found between 1.97 and

Table 5 Parameters of the fitted semivariograms for the soil erodibility factors obtained by using four different models

Soil erodibility factor	No. of observation	Best fit model	Nugget, C_0	Sill, $C_0 + C$	Range, A_0	$C_0/(C_0 + C)$ (%)	R^2
K_1	669	Spherical	0.002	0.008	1.97	25.00	0.925
K_2	669	Spherical	0.011	0.219	6.43	5.02	0.900
K_3	669	Spherical	0.018	0.131	7.07	13.74	0.963
K_4	669	Spherical	0.012	0.072	6.17	16.66	0.991

7.07 km and also did not exhibit any trend (Fig. 2). From the range values, it can be inferred that to predict the soil erodibility of Bundelkhand region, the maximum sampling distance should be 7.07 km. The Eq. 1 used only PSD data to calculate K_1 and showed the lowest range value; whereas, two more parameters (SPP and SOM) together with PSD triggered K_3 to have the highest spatial correlation among all the soil erodibility equations. K_2 and K_4 used PSD + SPP and PSD + SOM, respectively showed higher spatial correlation than K_1 but lower that K_3. Our findings confirmed the earlier result obtained by Saygm et al. (2011) that the range of influence become larger as the number of parameters for calculating the soil susceptibility to erosion increases.

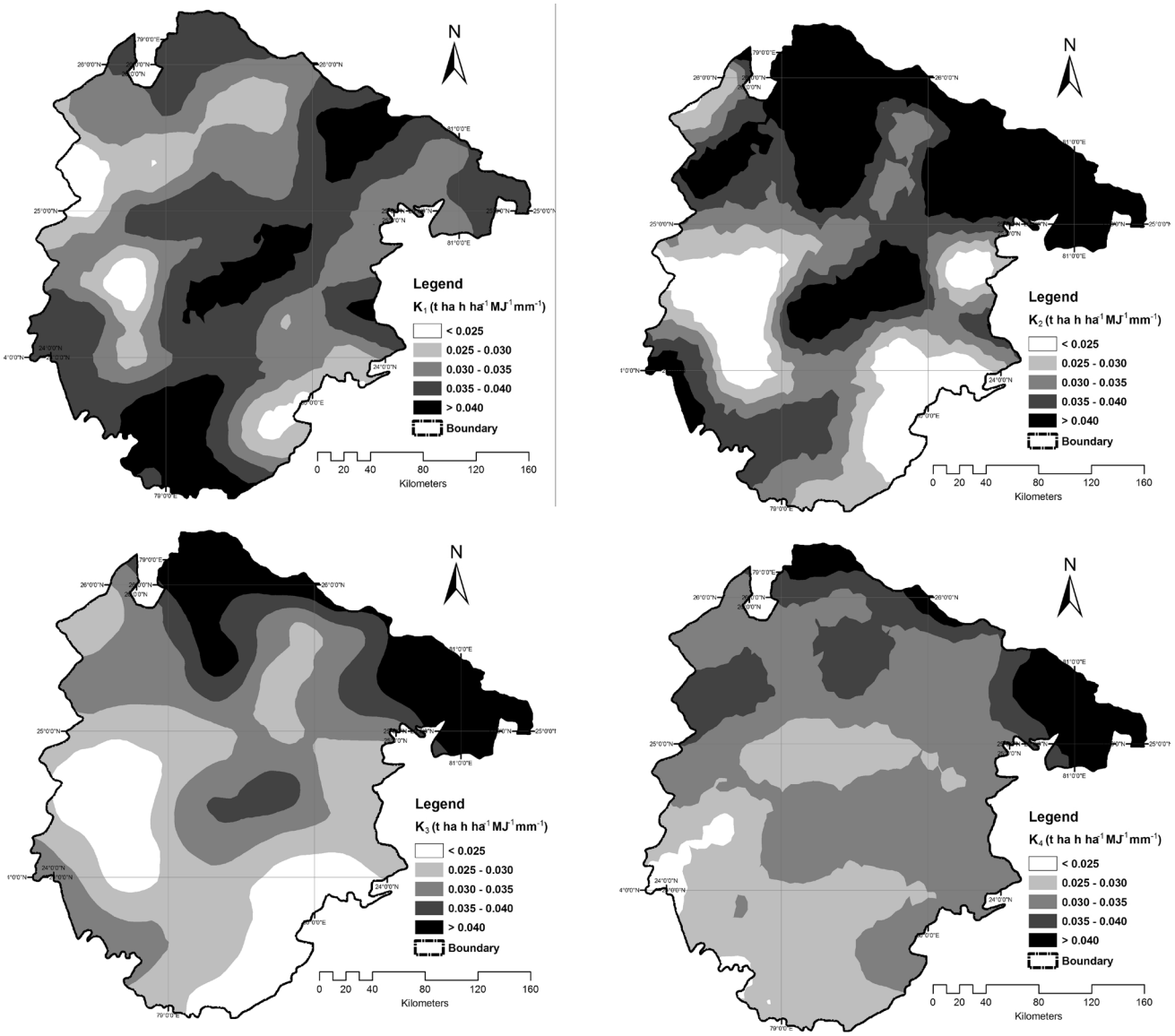

Fig. 3 Map displaying the spatial variation of soil erodibility factor in the Bundelkhand region obtained using four different models

Table 6 Error statistics of the soil erodibility factors obtained by using four different models

Soil erodibility factor	K_1	K_2	K_3	K_4
Mean error	7.32×10^{-4}	-3.56×10^{-5}	-1.03×10^{-4}	-3.83×10^{-6}
Root mean square error	0.015	0.011	0.008	0.006
Average standard error	0.025	0.013	0.005	0.009
Mean standardized error	0.023	0.010	0.003	0.007
Root mean square standardized error	0.775	0.872	1.074	0.976

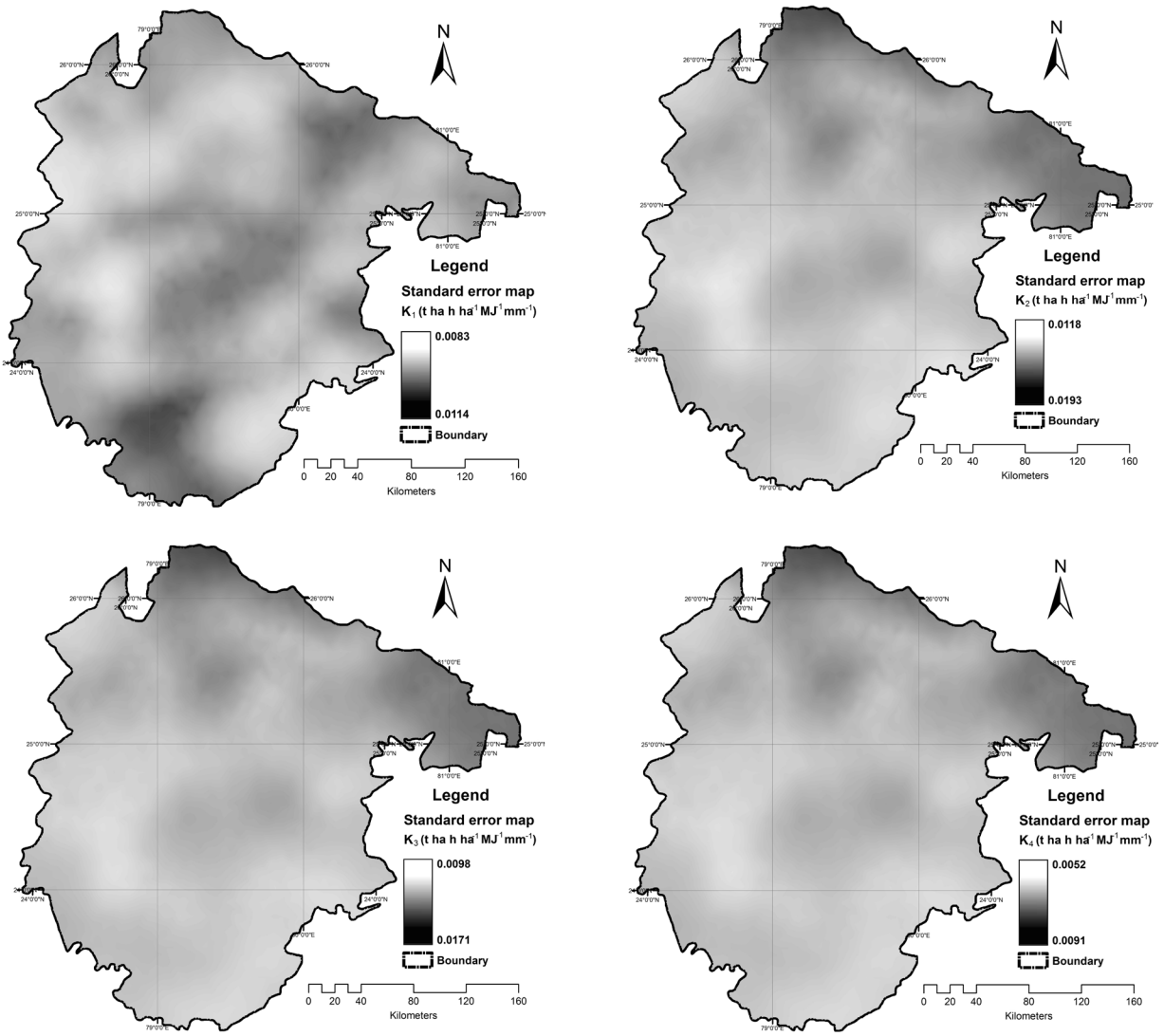

Fig. 4 Error maps of soil erodibility factor in the Bundelkhand region obtained using four different models

Spatial map of soil erodibility factors

The spatial patterns of soil erodibility obtained through four different models are presented in Fig. 3. Ordinary kriging (OK) interpolation method was used to generate the surface maps. The general trend was that lower soil erodibility was observed in western and southeastern part and higher soil erodibility was observed in the northern part of the study area. The northern part of Bundelkhand is called *UP-Bundelkhand*, situated on the southern bank of the *Yamuna* river and intensively cultivated. The intensive cultivation triggered the dominance of silt particles and lack of SOM in the soil system. This eventually led to the proneness to soil erosion. The

southern part of Bundelkhand, called *MP-Bundelkhand* is bestowed with huge forest land. Higher SOM at woodlands reduced the risk of soil erosion. Apart from these general trends there were differences in the interpolated maps due to the differences in the input parameters of different erodibility models. When SPP has been incorporated in the soil erodibility model K_2, it brought some additional area under high erosion risks which were otherwise under low erosion risk as depicted by model K_1. The areal extent of high erosion risk as depicted by models K_1 and K_2 was drastically reduced to moderate and low risk area when calculated through the models K_3 and K_4. The incorporation of SOM in the models K_3 and K_4 led to the reduction of high erosion risk area. This suggested that SOM, which was used by Eqs. 4 and 5 as a predictor parameter for K_3 and K_4 and not used by Eqs. 1 and 3 for K_1 and K_2, together with PSD was the critical variable to determine the RUSLE-K factor. Similar findings were also observed by Saygm et al. (2011) in Turkey. Land use types played the most prominent role in determining the variation of soil properties and thereby dictated the risk of soil erosion.

Performance of interpolation method

The performance of the ordinary kriging interpolation method was analyzed through cross validation of the observed and predicted values. To ascertain the predictability of the developed semivariogram models, the prediction error statistics were estimated (Table 6). For all the models, the error terms, ME, MSE, ASE, and RMSE were close to zero and RMSSE were close to one. This indicated that the ordinary kriging interpolation method was adequate and reliable to predict the spatial distribution of soil erodibility. Out of the four models, the model developed by Torri et al. (1997) performed best in the study area, followed by the Wischmeir and Smith (1978) model. One noteworthy finding was that the ME values of K_2, K_3 and K_4 were negative (Table 6). This was not an unusual result, considering the unbiased nature of the geostatistical methods. The negative ME suggested that the theoretical model was overestimating the soil erodibility (i.e., observed <predicted).

To ascertain further reliability of the surface maps developed by OK, the standard error maps were also created using OK (Fig. 4). The error maps indicated that the interpolated surface maps to predict the spatial variation of soil erodibility were quite reliable and can be used for developmental purpose. Noteworthy finding was that higher error values were associated with the areas having low sampling density and where higher potential erosion risk was expected.

Conclusions

Geospatial upscaling of soil erodibility factor, calculated from four commonly used models, which differed from each other according to their input parameters, was done to identify the suitability of the models. Soil erodibility varied under various land uses, depending upon the soil properties. The soil erodibility factors of woodlands and grasslands were lower than croplands and fallowlands, which were subjected to human induced degradation. Fibrous root systems coupled with coarser soil particles in the grasslands and higher sand and SOM content in the woodlands protect the soils from erosion. The spatial patterns of soil erodibility factors obtained from the models were successfully acquired over the study area and quite reliable. These can be used for developmental purpose and for planning from the perspective on land degradation assessment. It can also be concluded that along with the intrinsic soil properties, the dynamic soil properties, those changes in land use, influence the spatial prediction of soil erodibility factor. The model which used SOM along with PSD agreed better with the variations in land use to predict surface variation of soil erodibility factor.

References

Basaran M, Erpul G, Ozcan AU (2008) Variation of macro-aggregate stability and organic matter fractions in the basin of Saraykoy II Irrigation Dam, Cankiri, Turkey. Fresen Environ Bull 17:224–239

Baskan O, Cebel H, Akgul S, Erpul G (2010) Conditional simulation of USLE/RUSLE soil erodibility factor by geostatistics in a Mediterranean Catchment, Turkey. Environ Earth Sci 60:1179–1187

Bathrellos GD, Papanastassiou KG, Skilodimou HD, Papanastassiou D, Chousianitis KG (2012) Potential suitability for urban planning and industry development by using natural hazard maps and geological–geomorphological parameters. Environ Earth Sci 66:537–548

Bathrellos GD, Papanastassiou KG, Skilodimou HD, Skianis GA, Chousianitis KG (2013) Assessment of rural community and agricultural development using geomorphological-geological factors and GIS in the Trikala prefecture (Central Greece). Stoch Env Res Risk A 27:573–588

Bayramin I, Basaran M, Erpul G, Canga MR (2008) Assessing the effects of land use changes on soil sensitivity to erosion in a highland ecosystem of semi-arid Turkey. Environ Monit Assess 140:249–265

Botterweg P, Leek R, Romstad E, Vatn A (1998) The EUROSEM-GRIDSEM modelling system for erosion analyses under different natural and economic conditions. Ecol Model 108:115–129

Burgess TM, Webster R (1980) Optimal interpolation and isarithm mapping of soil properties: I. The semivariogram and punctual kriging. J Soil Sci 31:315–331

Buttafuoco G, Conforti M, Aucelli PPC, Robustelli G, Scarciglia F (2012) Assessing spatial uncertainty in mapping soil erodibility

factor using geostatistical stochastic simulation. Environ Earth Sci 66:1111–1125
Cambardella CA, Moorman TB, Novak JM, Parkin TB, Karlen DL, Turco RF, Konopka AE (1994) Field scale variability of soil properties in Central Iowa soils. Soil Sci Soc Am J 58: 1501–1511
Castrignano A, Buttafuoco G, Canu A, Zucca C, Madrau S (2008) Modeling spatial uncertainty of soil erodibility factor using joint stochastic simulation. Land Degrad Dev 19:198–213
Cerri CEP, Bernoux M, Chaplot V, Volkoff B, Victoria RL, Melillo JM, Paustian K, Cerri CC (2004) Assessment of soil property spatial variation in an Amazon pasture: basis for selecting agronomic experimental area. Geoderma 123:51–68
Chai X, Shen C, Yuan X, Huang Y (2008) Spatial prediction of soil organic matter in the presence of different external trends with REML-EBLUP. Geoderma 148:159–166
Chen X, Zhou J (2013) Volume-based soil particle fractal relation with soil erodibility in a small watershed of purple soil. Environ Earth Sci 70:1735–1746
Chen X, Zhang Z, Chen X, Shi P (2009) The impact of land use and land cover changes on soil moisture and hydraulic conductivity along the karst hillslopes of southwest China. Environ Earth Sci 59:811–820
Douaik A, Meirvenne MV, Tibor TT (2005) Soil salinity mapping using spatio-temporal kriging and Bayesian maximum entropy with interval soft data. Geoderma 128:234–248
Herbst M, Diekkrüger B, Vereecken H (2006) Geostatistical co-regionalization of soil hydraulic properties in a micro-scale catchment using terrain attributes. Geoderma 132:206–221
Journel AG, Huijbregts CS (1978) Mining geostatistics. Academic, New York, p 600
Klein J, Jarva J, Kamenetsky DF, Bogatyrev I (2013) Integrated geological risk mapping: a qualitative methodology applied in St. Petersburg, Russia. Environ Earth Sci 70:1629–1645
Klute A, Dirksen C (1986) Hydraulic conductivity and diffusivity: laboratory methods. In: Klute A (ed) Methods of soil analysis, part 1: Physical and mineralogical methods, 2nd edn. American Society of Agronomy, Madison, pp 687–734
Lee S (2004) Soil erosion assessment and its verification using the Universal Soil Loss equation and Geographic information system: a case study at Boun, Korea. Environ Geol 45:457–465
Lu D, Li G, Valladares GS, Batistella M (2004) Mapping soil erosion risk in Rondonia, Brazilian Amazonia: using RUSLE, remote sensing and GIS. Land Degrad Dev 15:499–512
Morgan RPC (1995) Soil erosion and conservation. Longman, White Plains
Mulengera MK, Payton RW (1999) Estimating the USLE-soil erodibility factor in developing tropical countries. Trop Agr 76:17–22
Nearing MA (2005) Soil erosion and conservation. In: Wainwright J, Mulligan M (eds) Environmental modelling: finding simplicity in complexity. Wiley, London, p 430
Parysow P, Wang G, Gerther G, Anderson A (2003) Spatial uncertainty analysis for mapping soil erodibility based on joint sequential simulation. Catena 53:65–78
Perovic V, Zivotic L, Kadovic R, Dordevic A, Jaramaz D, Mrvic V, Todorovic M (2013) Spatial modelling of soil erosion potential in a mountainous watershed of south-eastern Serbia. Environ Earth Sci 68:115–128
Piper CS (1966) Soil and plant analysis. Hans Publications, Bombay
Prasannakumar V, Shiny R, Geetha N, Vijith H (2011) Spatial prediction of soil erosion risk by remote sensing, GIS and RUSLE approach: a case study of Siruvani river watershed in Attapady valley, Kerala, India. Environ Earth Sci 64:965–972
Ratha Krishnan P (2008) Special plantation drive—towards livelihood security in Bundelkhand,Uttar Pradesh. Curr Sci India 95:708
Ravi S, Breshears DD, Huxman TE, D'Odoric P (2010) Land degradation in drylands: interactions among hydrologic-aeolian erosion and vegetation dynamics. Geomorphology 116:236–245
Renard KG, Foster GR, Weesies GA, McCool DK, Yoder DC (1997) Predicting soil erosion by water: a guide to conservation planning with the revised universal soil loss equation RUSLE. US Department of Agriculture, Agriculture Handbook 703, Government Printing Office, SSOP, Washington, D.C., p 404. ISBN: 0-16-048938-5
Rezapour S (2014) Response of some soil attributes to different land use types in calcareous soils with Mediterranean type climate in north-west of Iran. Environ Earth Sci 71:2199–2210
Romkens MJM, Prasad SN, Poesen JWA (1986) Soil erodibility and properties. In: Proceedings. 13th congress, International soil science society (vol 5, pp 492–504), Germany: Hamburg
Rozos D, Skilodimou HD, Loupasakis C, Bathrellos GD (2013) Application of the revised universal soil loss equation model on landslide prevention. An example from N. Euboea (Evia) Island, Greece. Environ Earth Sci 70:3255–3266
Sarangi A, Cox CA, Madramootoo CA (2005) Geostatistical methods for prediction of spatial variability of rainfall in a mountainous region. T ASAE 48:943–954
Saygm SD, Basaran M, Ozcan AU, Dolarslan M, Timur OB, Yilman FE, Erpul G (2011) Land degradation assessment by geo-spatially modeling different soil erodibility equations in a semi-arid catchment. Environ Monit Assess 180:201–215
Saygm SD, Ozcan AU, Basaran M, Timur OB, Dolarslan M, Yilman FE, Erpul G (2014) The combined RUSLE/SDR approach integrated with GIS and geostatistics to estimate annual sediment flux rates in the semi-arid catchment, Turkey. Environ Earth Sci 71:1605–1618
Seager R, Ting M, Held I, Kushnir Y, Lu J, Vecchi G, Huang H, Harnik N, Leetmaa A, Lau N, Li C, Velez J, Naik N (2007) Model projections of an imminent transition to a more arid climate in southwestern North America. Science 316:1181–1184
Shepherd TG, Newman RH, Ross CW, Dando JL (2001) Tillage induced changes in soil structure and soil organic matter fraction. Aust J Soil Res 39:465–489
Shirazi MA, Boersma L (1984) A unifying quantitative analysis of soil texture. Soil Sci Soc Am J 48:142–147
Shirazi MA, Boersma L, Hart W (1988) A unifying analysis of soil texture: improvement of precision and extension of scale. Soil Sci Soc Am J 52:181–190
Singh MJ, Khera KL (2009) Physical indicators of soil quality in relation to soil erodibility under different land uses. Arid Land Res Manag 23:152–167
Singh R, Phadke VS (2006) Assessing soil loss by water erosion in Jamni River Basin, Bundelkhand region, India, adopting universal soil loss equation using GIS. Curr Sci India 90: 1431–1435
Smith RE, Goodrich DC, Quinton JN (1995) Dynamic, distributed simulation of watershed-erosion: the Kineros2 and Eurosem models. J Soil Water Conserv 50:517–520
Soil Survey Staff (1996) Soil survey laboratory methods manual (No. 42, Version 3.0). Soil Survey Investigations Reports, Lincoln: USDA-NRCS
Sparovek G, Bacchi OOS, Schnug E, Ranieri SBL, Maria ICD (2000) Comparison of three water erosion prediction methods (137Cs, WEPP, USLE) in the southeast Brazilian sugarcane production. J Agric Trop Subtrop 101:107–118
Terranova O, Antronico L, Coscarelli R, Iaquinta P (2009) Soil erosion risk scenarios in the Mediterranean environment using

RUSLE and GIS: an application model for Calabria (southern Italy). Geomorphology 112:228–245

Tiwari SP, Narayan D (2010) Soil and water conservation measures for Bundelkhand region. In: Kokate KD (eds) Extension strategy for Bundelkhand region. Zonal project directorate, zone-IV (ICAR), Kanpur: 48–57

Torri D, Poesen J, Borselli L (1997) Predictability and uncertainty of the soil erodibility factor using a global dataset. Catena 31:1–22

Walkley A, Black IA (1934) An examination of the Degtjareff method for determining soil organic matter and a proposed modification of the chromic acid titration method. Soil Sci 37:29–38

Wang G, Gertner G, Liu X, Anderson A (2001) Uncertainty assessment of soil erodibility factor for revised universal soil loss equation. Catena 46:1–14

Wischmeir WH, Smith DD (1978) Predicting rainfall erosion losses (No. 537). USDA, Agricultural Service Handbook. Washington, DC

Youssef AM, Maerz NH (2013) Overview of some geological hazards in the Saudi Arabia. Environ Earth Sci 70:3115–3130